

# 6

## Electroweak Interactions

We have already discussed some aspects of weak and electromagnetic interactions when we discussed nuclear stability in Chapter 2 and again when we introduced the basic properties of leptons in Chapter 3. In this chapter we will consider wider aspects of the weak interaction and also its unification with electromagnetism to produce the spectacularly successful *electroweak theory*.

### 6.1 Charged and Neutral Currents

Like the strong and electromagnetic interactions, the weak interaction is also associated with elementary spin-1 bosons, which act as ‘force carriers’ between quarks and/or leptons. Until 1973 all observed weak interactions were consistent with the hypothesis that they were mediated by the exchange of the charged bosons  $W^\pm$  only. However, in the 1960s, a theory was developed which unified electromagnetic and weak interactions in a way that is often compared with the unification of electric and magnetic interactions by Maxwell a century earlier. This new theory made several remarkable predictions, including the existence of the heavy neutral vector boson  $Z^0$  and of weak reactions arising from its exchange. The latter processes are called *neutral current* reactions (the word neutral referring to the charge of the exchanged particle) to distinguish them from the so-called *charged current* reactions arising from charged  $W^\pm$  boson exchange. In particular, neutral current reactions of the type  $\nu_\mu + N \rightarrow \nu_\mu + X$  were predicted to occur via the mechanism of Figure 6.1, where  $N$  is a nucleon and  $X$  is any set of hadrons allowed by the conservation laws. Although difficult to detect, such reactions were first observed in a bubble chamber experiment in 1973.

The prediction of the existence and properties of neutral currents, prior to their discovery, is only one of many remarkable successes of the unified theory of electromagnetic and weak interactions. Others include the prediction of the existence of the charmed quark, prior to its discovery in 1974 and the prediction

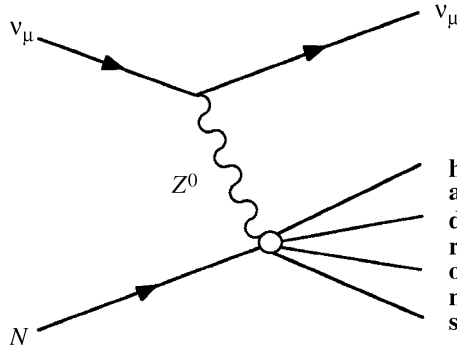


**Figure 6.1** Feynman diagram for the weak neutral current reaction  $\nu_\mu + N \rightarrow \nu_\mu + X$

of the masses of the  $W^\pm$  and  $Z^0$  bosons prior to the long-awaited detection of these particles in 1983. In general, the theory is in agreement with all data on both weak and electromagnetic interactions, which are now referred to collectively as the *electroweak interaction*, in the same way that electric and magnetic interactions are referred to collectively as electromagnetic interactions. Furthermore, the theory predicts the existence of a new spin-0 boson, the so-called *Higgs boson*, which is associated with the origin of particle masses within the model. This was mentioned in passing in earlier chapters. Although a detailed discussion of the Higgs boson is beyond the scope of this book, there is a brief discussion of the role of this very important particle in Chapter 9.

The new unification only becomes manifest at high energies, and at low energies weak and electromagnetic interactions can still be clearly separated. This follows from the general form of the amplitude Equation (1.41):

$$F(\mathbf{q}^2) = \frac{-g^2 \hbar^2}{|\mathbf{q}|^2 + M_X^2 c^2}, \quad (6.1)$$

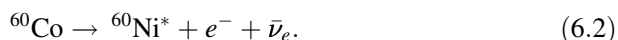
where  $M_X^2$  is the mass of the exchanged particle and  $g$  is the appropriate coupling. For weak interactions,  $M_X = M_{W,Z} \approx 80 \text{ GeV}/c^2$  and for the electromagnetic interaction  $M_X = M_\gamma = 0$ . Thus, even with  $g_{\text{weak}} \sim g_{\text{em}}$ , the amplitudes for the two interactions will only become of comparable size for  $|\mathbf{q}|^2 \sim M_X^2 c^2$ , i.e. at high energies. We therefore start by considering the weak interaction at low energies and deduce some of its general properties that are valid at all energies. Later we will consider how unification arises and some of its consequences.

## 6.2 Symmetries of the Weak Interaction

In this section we will discuss the parity ( $P$ ) and charge conjugation ( $C$ ) operators, which were introduced in Chapter 1. These are conserved in the strong and

electromagnetic interactions. The first indication that parity might be violated in weak interactions came from observations on the pionic decays of  $K$ -mesons, i.e.  $K \rightarrow \pi\pi$  and  $K \rightarrow \pi\pi\pi$ ,<sup>1</sup> and these led Lee and Yang in 1956 to make a thorough study of all previous experiments in which parity conservation had been assumed or apparently proved. They came to the startling conclusion that there was in fact no firm evidence for parity conservation in weak interactions; and they suggested experiments where the assumption could be tested.<sup>2</sup> This led directly to the classic demonstration of parity violation from a study of the  $\beta$ -decay of polarized  $^{60}\text{Co}$  nuclei. We shall just describe the principles of this experiment.<sup>3</sup>

The experiment was done in 1957 by Wu and co-workers, who placed a sample of  $^{60}\text{Co}$  inside a magnetic solenoid and cooled it to a temperature of 0.01 K. At such temperatures, the interaction of the magnetic moments of the nuclei with the magnetic field overcomes the tendency to thermal disorder, and the nuclear spins tend to align parallel to the field direction. The polarized  $^{60}\text{Co}$  nuclei produced in this way decay to an excited state of  $^{60}\text{Ni}$  by the  $\beta$ -decay



Parity violation was established by the observation of a ‘forward–backward decay asymmetry’, i.e. the fact that fewer electrons were emitted in the forward hemisphere than in the backward hemisphere with respect to the spins of the decaying nuclei.

We can show that this implies parity violation as follows. The parity transformation reverses all particle momenta  $\mathbf{p}$  while leaving their orbital angular momenta  $\mathbf{r} \times \mathbf{p}$ , and by analogy their spin angular momenta, unchanged. Hence in the rest frame of the decaying nuclei its effect is to reverse the electron velocity while leaving the nuclear spins unchanged, as shown in Figure 6.2. Parity invariance would then require that the rates for the two processes Figure 6.2(a) and Figure 6.2(b) were equal, so that equal numbers of electrons would be emitted in the forward and backward hemispheres with respect to the nuclear spins, in contradiction to what was observed. The discovery of parity violation was a watershed in the history of weak interactions because the effect is large, and an understanding of weak interactions is impossible if it is neglected.

The charge conjugation operator  $C$  changes all particles to antiparticles and as we will see presently is also not conserved in weak interactions. In examining these operators, two interconnected themes will emerge. The first is that these effects have their origin in the spin dependence of weak interactions; the second is

<sup>1</sup>Two particles, called at that time  $\tau$  and  $\theta$ , were observed to decay via the weak interaction to  $\pi\pi$  and  $\pi\pi\pi$  final states, respectively, which necessarily had different final-state parities. However, the  $\tau$  and  $\theta$  had properties, including the near equality of their masses, which strongly suggested that they were in fact the same particle. Analysis of the ‘ $\tau$ – $\theta$  puzzle’ suggested that parity was not conserved in the decays.

<sup>2</sup>For their work on parity non-conservation, Chen Yang and Tsung-Dao Lee were awarded the 1957 Nobel Prize in Physics.

<sup>3</sup>This classic experiment is described in readable detail in Chapter 10 of Tr75.

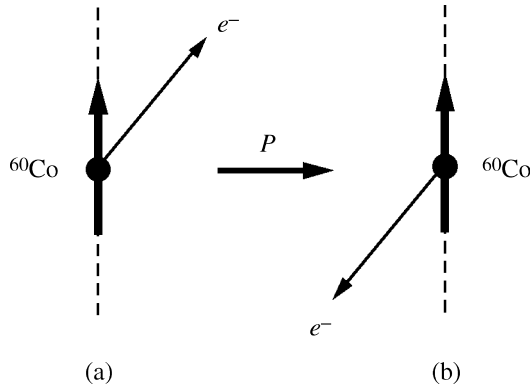


**Figure 6.2** Effect of a parity transformation on  $^{60}\text{Co}$  decay: the thick arrows indicate the direction of the spin of the  $^{60}\text{Co}$  nucleus, while the thin arrows show the direction of the electron's momentum

that while  $P$ -violation and  $C$ -violation are large effects, there is a weaker combined symmetry, called  $CP$ -invariance, which is almost exactly conserved. This has its most striking consequences for the decays of neutral mesons, which are also discussed below. We start by considering the  $P$  and  $C$  operators in more detail.

$C$ -violation and  $P$ -violation are both conveniently illustrated by considering the angular distributions of the electrons and positrons emitted in the decays

$$\mu^- \rightarrow e^- + \bar{\nu}_e + \nu_\mu \quad (6.3a)$$

and

$$\mu^+ \rightarrow e^+ + \nu_e + \bar{\nu}_\mu \quad (6.3b)$$

of polarized muons. In the rest frame of the decaying particle these were found to be of the form

$$\Gamma_{\mu^\pm}(\cos\theta) = \frac{1}{2}\Gamma_\pm \left[ 1 - \frac{\xi_\pm}{3}\cos\theta \right], \quad (6.4)$$

where  $\theta$  is the angle between the muon spin direction and the direction of the outgoing electron or positron, as shown in Figure 6.3(a). The quantities  $\xi_\pm$  are called the asymmetry parameters, and  $\Gamma_\pm$  are the total decay rates, or equivalently the inverse lifetimes, i.e.

$$\tau_\pm^{-1} \equiv \int_{-1}^{+1} d\cos\theta \Gamma_{\mu^\pm}(\cos\theta) = \Gamma_\pm, \quad (6.5)$$

as may easily be checked by direct substitution.

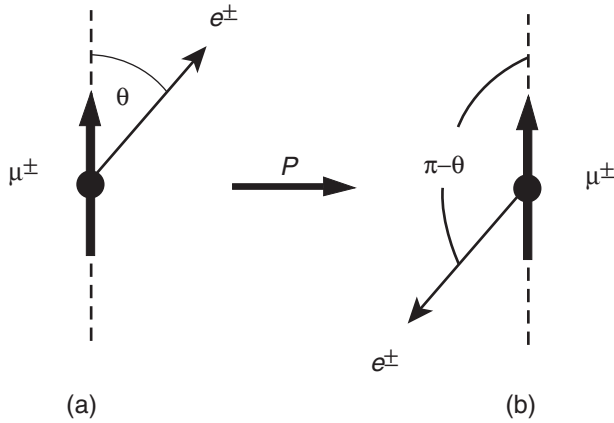


**Figure 6.3** Effect of a parity transformation on muon decays: the thick arrows indicate the direction of the muon spin, while the thin arrows indicate the direction of the electron’s momentum

We consider now the consequences of assuming parity and charge conjugation for these decays, starting with the latter as it is the simpler. Under charge conjugation,  $\mu^-$  decay converts to  $\mu^+$  decay.  $C$ -invariance then implies that the rates and angular distributions for these decays should be the same, i.e.

$$\Gamma_+ = \Gamma_- \quad (C\text{-invariance}) \tag{6.6}$$

and

$$\xi_+ = \xi_- \quad (C\text{-invariance}). \tag{6.7}$$

The parity transformation preserves the identity of the particles, but reverses their momenta while leaving their spins unchanged. Its effect on muon decay is shown in Figure 6.3, where we see that it changes the angle  $\theta$  to  $\pi - \theta$ , so that  $\cos \theta$  changes sign. Hence  $P$ -invariance implies

$$\Gamma_{\mu^\pm}(\cos \theta) = \Gamma_{\mu^\pm}(-\cos \theta) \quad (P\text{-invariance}). \tag{6.8}$$

Substituting Equation (6.4), leads to the prediction that the asymmetry parameters vanish,

$$\xi_\pm = 0 \quad (P\text{-invariance}). \tag{6.9}$$

Experimentally, the  $\mu^\pm$  lifetimes are equal to a very high level of precision, so that the prediction for the lifetimes is satisfied; but the measured values of the

asymmetry parameters are

$$\xi_- = -\xi_+ = 1.00 \pm 0.04, \quad (6.10)$$

which shows that both  $C$ -invariance and  $P$ -invariance are violated. The violation is said to be ‘maximal’, because the asymmetry parameters are defined to lie in the range  $-1 \leq \xi_{\pm} \leq 1$ .

In view of these results, a question that arises is: why do the  $\mu^+$  and  $\mu^-$  have the same lifetime if  $C$ -invariance is violated? The answer lies in the principle of  $CP$ -conservation, which states that the weak interaction is invariant under the combined operation  $CP$  even though both  $C$  and  $P$  are separately violated. The  $CP$  operator transforms particles at rest to their corresponding antiparticles at rest, and  $CP$ -invariance requires that these states should have identical properties. Thus, in particular, the masses of particles and antiparticles are predicted to be the same. Specifically, if we apply the  $CP$  operator to muon decays, the parity operator changes  $\theta$  to  $\pi - \theta$  as before, while the  $C$  operator changes particles to antiparticles. Hence  $CP$ -invariance alone implies that the condition obtained from  $P$ -invariance is replaced by the weaker condition

$$\Gamma_{\mu^+}(\cos \theta) = \Gamma_{\mu^-}(-\cos \theta). \quad (6.11)$$

Again, substituting Equation (6.4) into Equation (6.11), gives

$$\Gamma_+ = \Gamma_- \quad (CP\text{-invariance}), \quad (6.12)$$

implying equal lifetimes and also

$$\xi_+ = -\xi_- \quad (CP\text{-invariance}), \quad (6.13)$$

in agreement with the experimental results. Thus  $CP$ -invariance retains the symmetry between particles and antiparticles as observed by experiment, at least for  $\mu$ -decays. In fact  $CP$ -invariance has been verified in a wide variety of experiments involving weak interactions, and it is believed to be exact for purely leptonic processes (i.e. ones involving only leptons) and a very good approximation for those involving hadrons. (The only known violations will be discussed in Section 6.6.1.) Particles and antiparticles have the same masses and lifetimes even if  $CP$  is not conserved.

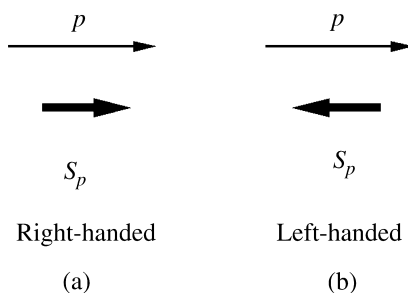
### 6.3 Spin Structure of the Weak Interactions

We turn now to the spin structure of the weak interactions, which is closely related to the symmetry properties discussed above. As this spin structure takes its simplest form for zero-mass particles, we will discuss the case of neutrinos and

antineutrinos first, assuming that they have zero mass for the purpose of this discussion.

### 6.3.1 Neutrinos

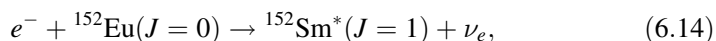
In discussing neutrinos, it is convenient to use the so-called *helicity states*, in which the spin is quantized along the direction of motion of the particle, rather than along some arbitrarily chosen ‘ $z$ -direction’. For a spin- $\frac{1}{2}$  particle, the spin component along the direction of its motion can be either  $+\frac{1}{2}$  or  $-\frac{1}{2}$  (in units of  $\hbar$ ), as illustrated in Figure 6.4, corresponding to positive or negative helicity respectively. These states are called *right-handed* or *left-handed*, respectively, since the spin direction corresponds to rotational motion in a right-handed or left-handed sense when viewed along the momentum direction.



**Figure 6.4** Helicity states of a spin- $\frac{1}{2}$  particle: the long thin arrows represent the momenta of the particles and the shorter thick arrows represent their spins

We will denote these states by a subscript R or L, so that, for example,  $\nu_L$  means a left-handed neutrino. The remarkable fact about neutrinos and antineutrinos, which only interact via the weak interaction, is that *only left-handed neutrinos  $\nu_L$  and right-handed antineutrinos  $\bar{\nu}_R$  are observed in nature*. This obviously violates  $C$ -invariance, which requires neutrinos and antineutrinos to have identical weak interactions. It also violates  $P$ -invariance, which requires the states  $\nu_L$  and  $\nu_R$  to also have identical weak interactions, since the parity operator reverses the momentum while leaving the spin unchanged and so converts a left-handed neutrino into a right-handed neutrino. It is, however, compatible with  $CP$ -invariance, since the  $CP$  operator converts a left-handed neutrino to a right-handed antineutrino, as illustrated in Figure 6.5.

The helicity of the neutrino was first measured in an ingenious experiment by Goldhaber and co-workers in 1958. Again, we will only discuss the principles of the experiment. They studied electron capture in  $^{152}\text{Eu}$ , i.e.



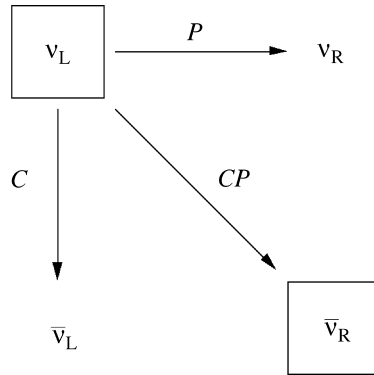
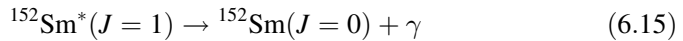
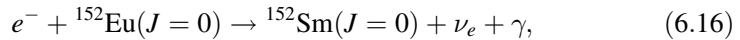


**Figure 6.5** Effect of  $C$ ,  $P$  and  $CP$  transformations; only the states shown in boxes are observed in nature

where the spins of the nuclei are shown in brackets. The excited state of samarium that is formed decays to the ground state by  $\gamma$ -emission



and it is these  $\gamma$ -rays which were detected in the experiment. In the first reaction (Equation (6.14)), the electrons are captured from the K-shell and the initial state has zero momentum, so that the neutrino and the  $^{152}\text{Sm}^*$  nucleus recoil in opposite directions. The experiment selected events in which the photon was emitted in the direction of motion of the decaying  $^{152}\text{Sm}^*$  nucleus, so that overall the observed reaction was



where the three final-state particles were co-linear, and the neutrino and photon emerged in opposite directions, as shown in Figure 6.6.

The helicity of the neutrino can then be deduced from the measured helicity of the photon by applying angular momentum conservation about the event axis to the overall reaction. In doing this, no orbital angular momentum is involved, because the initial electron is captured from the atomic K-shell and the final-state particles all move along the event axis. Hence the spin components of the neutrino and photon, which can be  $\pm\frac{1}{2}$  and  $\pm 1$  respectively, must add to give the spin component of the initial electron, which can be  $\pm\frac{1}{2}$ . This gives two possible spin configurations, as shown in Figures 6.6(a) and 6.6(b). In each case the photon and neutrino have the same helicities. In the actual experiment, the polarization of the photons was determined by studying their absorption in magnetized iron (which depends on the polarization of the photon) and the results obtained were consistent with the occurrence of left-handed neutrinos only, corresponding to Figure 6.6(a).

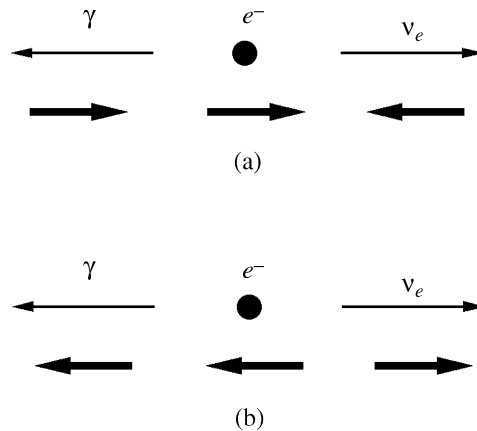


**Figure 6.6** Possible helicities of the photon and neutrinos emitted in the reaction  $e^- + {}^{152}\text{Eu}(J=0) \rightarrow {}^{152}\text{Sm}(J=0) + \nu_e + \gamma$  for those events in which they are emitted in opposite directions. Experiment selects configuration (a)

Later experiments have shown that only right-handed antineutrinos take part in weak interactions.

### 6.3.2 Particles with mass: chirality

To see the effect of the spin dependence in weak interactions involving particles with mass, we will look at the decays of the pion and muon which are, of course, examples of charged current reactions. The spin dependence is of a special form, called a  $V-A$  interaction. This name is derived from the behaviour under a parity transformation of the weak interaction analogue of the electromagnetic current. The letter  $\mathbf{V}$  denotes a *proper vector*, which is one whose direction is reversed by a parity transformation (an example is momentum  $\mathbf{p}$ ). The familiar electric current, to which photons couple, transforms as a proper vector under parity. Because parity is not conserved in weak interactions, the corresponding weak current, to which  $W^\pm$ -bosons couple, has in addition to a vector ( $\mathbf{V}$ ) component another component whose direction is unchanged by a parity transformation. Such a quantity is called an *axial-vector* ( $\mathbf{A}$ ) (an example of an axial-vector is orbital angular momentum  $\mathbf{L} = \mathbf{r} \times \mathbf{p}$ ). Since observables are related to the modulus squared of amplitudes, either term would lead by itself to parity conservation. Parity non-conservation is an interference effect between the two components.

Here we shall consider only the most important characteristic of this spin dependence, which is that the results discussed above for neutrinos, hold for all fermions in the ultra-relativistic limit. That is, in the limit that their velocities approach that of light, only left-handed fermions  $\nu_L$ ,  $e_L^-$  etc. and right-handed antifermions  $\bar{\nu}_R$ ,  $e_R^+$  etc. are emitted in charged current interactions. These

right-handed and left-handed particles are called *chiral* states and these are the eigenstates that take part in weak interactions. In general, chiral states are linear combinations of helicity states,<sup>4</sup> with the contributions of the ‘forbidden’ helicity states  $e_R^-$ ,  $e_L^+$  etc. suppressed by factors which are typically of the order of  $(mc^2/E)^2$ , where  $m$  is the appropriate fermion mass and  $E$  its energy. For massless neutrinos this is always a good approximation and chiral states and helicity states are identical. However, for particles with mass, it is only a good approximation for large energies  $E$ . These spin properties can be verified most easily for the electrons and muons emitted in weak decays, by directly measuring their spins. Here we shall assume them to hold and use them to understand some interesting features of pion and muon decays.

We start by considering the pion decay mode

$$\pi^+ \rightarrow \ell^+ + \nu_\ell. \quad (\ell = e, \mu) \quad (6.17)$$

In the rest frame of the decaying pion, the charged lepton and the neutrino recoil in opposite directions, and because the pion has zero spin, their spins must be opposed to satisfy angular momentum conservation about the decay axis. Since the neutrino (assumed to be zero mass) is left-handed, it follows that the charged lepton must also be left-handed, as shown in Figure 6.7, in contradiction to the expectations for a relativistic antilepton.

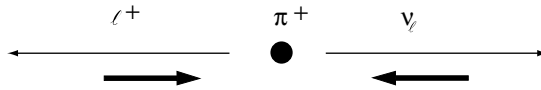


**Figure 6.7** Helicities of the charged leptons in pion decays: the short arrows denote spin vectors and the longer arrows denote momentum vectors

For the case of a positive muon this is unimportant, since it is easy to check that it recoils non-relativistically and so both chirality states are allowed. However, if a positron is emitted it recoils *relativistically*, implying that this mode is suppressed by a factor that we can estimate from the above to be of the order of  $(m_e/m_\pi)^2 \approx 10^{-5}$ . Thus the positron decay mode is predicted to be much rarer than the muonic mode. This is indeed the case, and the measured ratio

$$\frac{\Gamma(\pi^+ \rightarrow e^+ + \nu_e)}{\Gamma(\pi^+ \rightarrow \mu^+ + \nu_\mu)} = (1.218 \pm 0.014) \times 10^{-4} \quad (6.18)$$

is in excellent agreement with a full calculation that takes into account both the above suppression and the difference in the density-of-final states (i.e. the difference in the  $Q$ -values) for the two reactions.

<sup>4</sup>This is another example where linear combinations of states are the ones of physical interest; compare neutrino mixing (Section 3.1.3).

A second consequence of the chirality argument is that the muons emitted in pion decays are 100 per cent polarized (see Figure 6.7).<sup>5</sup> We have mentioned this earlier in connection with measuring the muon decay asymmetries. These have their origins in the spin structure of the interaction, as we shall illustrate for the highest-energy electrons emitted in the decay of the muon. These have energy

$$E = \frac{m_\mu c^2}{2} \left( 1 + \frac{m_e^2}{m_\mu^2} \right) \gg m_e c^2 \quad (6.19)$$

and correspond to decays in which the neutrino and antineutrino are both emitted in the direction opposite to the electron. This is illustrated in Figure 6.8 for the two simplest cases in which the electron is emitted in the muon spin direction (Figure 6.8(a)) and opposite to it (Figure 6.8(b)).

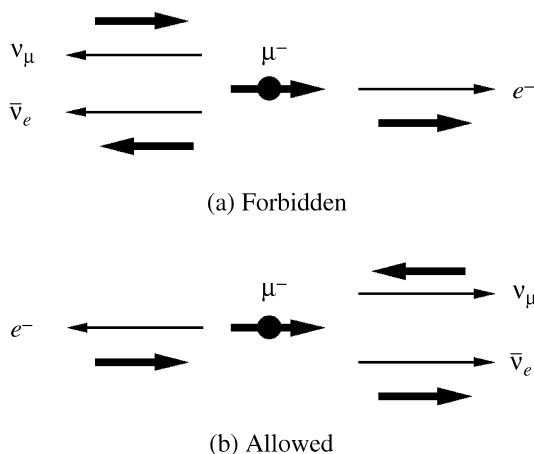


**Figure 6.8** Muon decays in which electrons of the highest possible energy are emitted: (a) in the muon spin direction, and (b) opposite to the muon spin direction

Since the neutrino and antineutrino have opposite helicities, the muon and electron must have the same spin component along the event axis in order to conserve angular momentum, implying the electron helicities shown in Figure 6.8. When combined with the fact that the relativistic electrons emitted must be left-handed, this implies that electrons cannot be emitted in the muon spin direction. We thus see that the spin structure of the interaction automatically gives rise to a forward-backward asymmetry in polarized muon decays. Of course not all the electrons have the maximum energy and the actual asymmetry, averaged over all electron energies, can only be calculated by using the full form of the **V-A**

<sup>5</sup>This is in the rest frame of the decaying pion and assumes that the neutrino has zero mass. The degree of polarization in the laboratory frame is a function of the muon momentum.

interaction.<sup>6</sup> The resulting prediction is in excellent agreement with the measured values.

Finally, we have seen in earlier chapters that there is increasing evidence that neutrinos are not strictly massless. How then can we ensure that the weak interactions only couple to  $\nu_L$  and  $\bar{\nu}_R$ ? To understand this we return to the Dirac equation, which was mentioned in Chapter 1. As was stated there, the solution of this equation for a massive spin- $\frac{1}{2}$  particle is in the form of a four-component spinor, whose components are interpreted as the two possible spin projections for the particle and its antiparticle of a given energy (see Section 1.2 and Equation (1.4)). However, in the case of a massless fermion the Hamiltonian of Equation (1.2) consists only of a spin projection term and there is a simpler solution of the Dirac equation consisting of two independent two-component wavefunctions. If we assume for definiteness the case of neutrinos (assumed to be massless), then these would correspond to the pairs  $(\nu_L, \bar{\nu}_R)$  and  $(\nu_R, \bar{\nu}_L)$ . This observation was first made by Weyl in 1929, but was rejected as unphysical because under a parity transformation  $\nu_L \rightarrow \nu_R$  (see Figure 6.5) and hence the interaction would not be invariant under parity. However, we now know that parity is not conserved in the weak interactions, so this objection is no longer valid. A possible solution is therefore to make the neutrino its own antiparticle. In this case  $(\nu_L, \bar{\nu}_R)$  are identified as two helicity components of a four-component spinor and the other two components  $(\nu_R, \bar{\nu}_L)$ , if they exist, can then be a fermion of a different mass. This scheme is due to Majorana and is very different to the structure of a spinor describing a massive spin- $\frac{1}{2}$  fermion such as an electron. A test of this idea would be the observation of neutrinoless double  $\beta$ -decay, such as that given in Equation (3.37), which is only possible if  $\nu_e \equiv \bar{\nu}_e$ .

## 6.4 $W^\pm$ and $Z^0$ Bosons

The three intermediate vector bosons mediating weak interactions, the two charged bosons  $W^+$  and  $W^-$  and the neutral  $Z^0$ , were all discovered at CERN in 1983 in the reactions

$$\bar{p} + p \rightarrow W^+ + X^-, \quad \bar{p} + p \rightarrow W^- + X^+, \quad \text{and} \quad \bar{p} + p \rightarrow Z^0 + X^0, \quad (6.20)$$

where  $X^\pm$  and  $X^0$  are arbitrary hadronic states allowed by the conservation laws. The beams of protons and antiprotons were supplied by a proton-antiproton collider, which was specifically built for this purpose. At the time it had proton and antiproton beams with maximum energies of 270 GeV each, giving a total centre-of-mass energy of 540 GeV. Two independent experiments were mounted (called

<sup>6</sup>See, for example, Chapter 12 of Ha84.

UA1 and UA2), both of which were examples of the ‘layered’ detector systems that were discussed in Chapter 4.<sup>7</sup> One of the main problems facing the experimenters was that for each event in which a  $W^\pm$  or  $Z^0$  is produced and decays to leptons, there were more than  $10^7$  events in which hadrons alone are produced and so the extraction of the signal required considerable care.

In contrast to the zero mass photons and gluons, the  $W^\pm$  and  $Z^0$  bosons are both very massive particles, with measured masses

$$M_W = 80.6 \text{ GeV}/c^2, \quad M_Z = 91.2 \text{ GeV}/c^2, \quad (6.21)$$

while their lifetimes are about  $3 \times 10^{-25}$  s. Their dominant decays lead to jets of hadrons, but the leptonic decays

$$W^+ \rightarrow \ell^+ + \nu_\ell, \quad W^- \rightarrow \ell^- + \bar{\nu}_\ell \quad (6.22)$$

and

$$Z^0 \rightarrow \ell^+ + \ell^-, \quad Z^0 \rightarrow \nu_\ell + \bar{\nu}_\ell, \quad (6.23)$$

where  $\ell = e, \mu$  or  $\tau$  as usual, are also important. The particles are detected as resonance-like enhancements in plots of the invariant mass of suitable final states seen in reactions such as Equation (6.20).<sup>8</sup>

We have seen that an important feature of an exchange interaction is its strength. As in the case of electromagnetism, Feynman diagrams for weak interactions are constructed from fundamental three-line vertices. Those for lepton– $W^\pm$  interactions are shown in Figure 6.9.

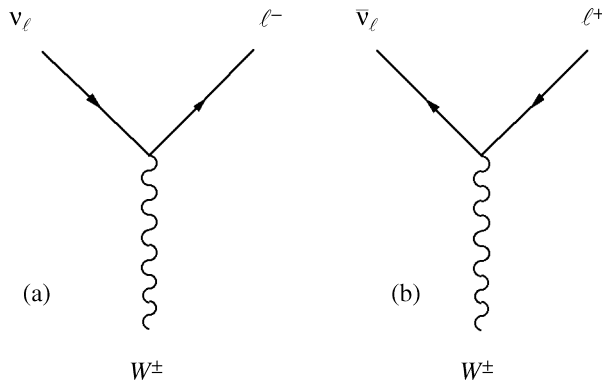


**Figure 6.9** The two basic vertices for  $W^\pm$ -lepton interactions

<sup>7</sup>Simon van der Meer lead the team that built the accelerator and Carlo Rubbia lead the UA1 experimental team that subsequently discovered the bosons. They shared the 1984 Nobel Prize in Physics for their work.

<sup>8</sup>A more detailed description of the UA1 experiment is given in, for example, Section 8.1 of Ma97.

At each vertex a boson is emitted or absorbed; while both fermion lines belong to the same generation  $\ell = e, \mu$  or  $\tau$ , with one arrow pointing inwards and one outwards to guarantee conservation of each lepton number  $N_e, N_\mu$  and  $N_\tau$ . Finally, associated with each vertex is a dimensionless parameter with the same value

$$\alpha_W = g_W^2/4\pi\hbar c \approx 1/400 \quad (6.24)$$

at high energies for *all three generations* (because of lepton universality). This constant is the weak analogue of the fine structure constant  $\alpha \approx 1/137$  in electromagnetic interactions, with  $g_W$  the weak analogue of the electronic charge  $e$  in appropriate units.

We see from the above that, despite its name, the weak interaction has a similar intrinsic strength to the electromagnetic interaction. Its apparent weakness in many low-energy reactions, is solely a consequence of its short range, which arises because the exchange bosons are heavy. From Equation (6.1) we see that the scattering amplitude has a denominator that contains the squared mass of the exchanged particle and so at energies where the de Broglie wavelengths  $\lambda = h/p$  of the particles are large compared with the range of the weak interaction, which is an excellent approximation for all lepton and hadron decays, the range can be neglected altogether. In this approximation the weak interaction becomes a *point* or *zero range* interaction, whose effective interaction strength can be shown to be

$$\alpha_{\text{eff}} = \alpha_W (\bar{E}/M_W c^2)^2, \quad \bar{E} \ll M_W c^2, \quad (6.25)$$

where  $\bar{E}$  is a typical energy scale for the process in question. (For example in muon decay it would be the mass of the muon.) Thus we see that the interaction is both weak and very energy dependent at ‘low energies’, but becomes comparable in strength with the electromagnetic interaction at energies on the scale of the  $W$ -boson mass.

## 6.5 Weak Interactions of Hadrons

The weak decays of hadrons are understood in terms of basic processes in which  $W^\pm$  bosons are emitted or absorbed by their constituent quarks. In this section we will consider both decays and scattering processes, starting with the former.

### 6.5.1 Semileptonic decays

A typical semileptonic decay (i.e. one that involves both hadrons and leptons) is that of the neutron, which at the quark level is

$$d \rightarrow u + e^- + \bar{\nu}_e, \quad (6.26)$$

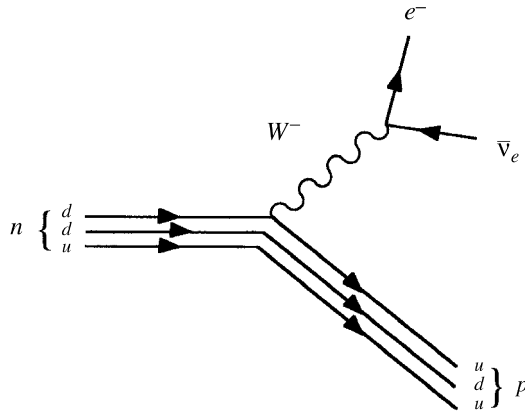


**Figure 6.10** Quark diagram for the decay  $n \rightarrow pe^- \bar{\nu}_e$

as illustrated in Figure 6.10, where the other two quarks play the role of spectators. Similarly, in the pion decay process

$$\pi^- (d\bar{u}) \rightarrow \mu^- + \bar{\nu}_\mu \quad (6.27)$$

the initial quarks annihilate to produce a  $W$  boson as shown in Figure 6.11. However, the weak interactions of quarks are more complicated than those of leptons, and are best understood in terms of two ideas: *lepton–quark symmetry*, and *quark mixing*.

For simplicity, we will look firstly at the case of just two generations of quarks and leptons. In this case, lepton–quark symmetry asserts that the first two generations of quarks

$$\begin{pmatrix} u \\ d \end{pmatrix} \quad \text{and} \quad \begin{pmatrix} c \\ s \end{pmatrix} \quad (6.28)$$

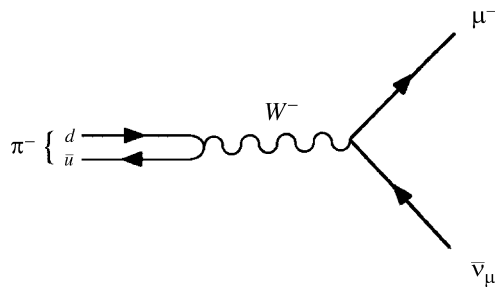


**Figure 6.11** Quark diagram for the process  $\pi^- \rightarrow \mu^- + \bar{\nu}_\mu$

and the first two generations of leptons

$$\begin{pmatrix} \nu_e \\ e^- \end{pmatrix} \quad \text{and} \quad \begin{pmatrix} \nu_\mu \\ \mu^- \end{pmatrix} \quad (6.29)$$

have *identical* weak interactions. That is, one can obtain the basic  $W^\pm$  quark vertices by making the replacements  $\nu_e \rightarrow u$ ,  $e^- \rightarrow d$ ,  $\nu_\mu \rightarrow c$ ,  $\mu^- \rightarrow s$  in the basic  $W^\pm$  lepton vertices, leaving the coupling constant  $g_W$  unchanged. The resulting  $W^\pm$  quark vertices are shown in Figure 6.12.

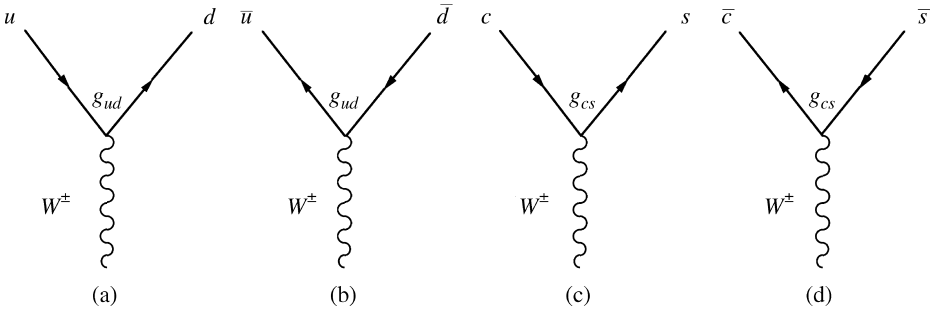


**Figure 6.12** The  $W^\pm$  quark vertices obtained from quark–lepton symmetry, without quark mixing

Quark symmetry in the simple form stated above then implies that the fundamental processes  $d + \bar{u} \rightarrow W^-$  and  $s + \bar{c} \rightarrow W^-$  occur with the *same* couplings  $g_W$  as the corresponding leptonic processes, i.e. in Figure (6.12) we have  $g_{cs} = g_{ud} = g_W$ , while the processes  $s + \bar{u} \rightarrow W^-$  and  $d + \bar{c} \rightarrow W^-$  are forbidden. This works quite well for many reactions, like the pion decay  $\pi^- \rightarrow \mu^- + \bar{\nu}_\mu$ , but many decays that are forbidden in this simple scheme are observed to occur, albeit at a rate which is suppressed relative to the ‘allowed’ decays. An example of this is the kaon decay  $K^- \rightarrow \mu^- + \bar{\nu}_\mu$ , which requires a  $s + \bar{u} \rightarrow W^-$  vertex, which is not present in the above scheme.

All these suppressed decays can be successfully incorporated into the theory by introducing *quark mixing*. According to this idea, the  $d$  and  $s$  quarks participate in the weak interactions via the linear combinations

$$d' = d \cos \theta_C + s \sin \theta_C \quad (6.30a)$$

and

$$s' = -d \sin \theta_C + s \cos \theta_C, \quad (6.30b)$$

where the parameter  $\theta_C$  is called the *Cabibbo angle*.<sup>9</sup> That is, lepton–quark symmetry is assumed to apply to the doublets

$$\begin{pmatrix} u \\ d' \end{pmatrix} \quad \text{and} \quad \begin{pmatrix} c \\ s' \end{pmatrix}. \quad (6.31)$$

This then generates new vertices previously forbidden. For example, the  $usW$  vertex required for the decay  $K^- \rightarrow \mu^- + \bar{\nu}_\mu$  arises from the interpretation of the  $ud'W$  vertex shown in Figure 6.13. In a similar way a new  $cdW$  vertex is also generated.

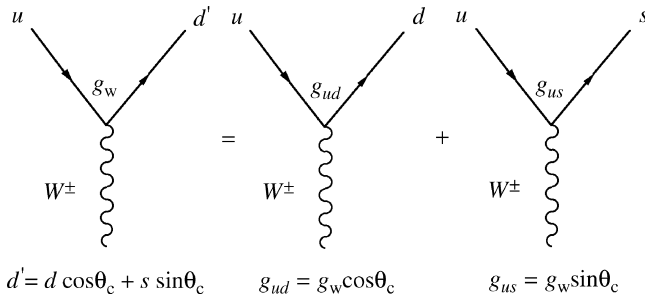


**Figure 6.13** The  $ud'W$  vertex and its interpretation in terms of  $udW$  and  $usW$  vertices

Quark mixing enables theory and experiment to be brought into good agreement by choosing a value  $\theta_C \approx 13^\circ$  for the Cabibbo angle. One then finds that the rates for the previously ‘allowed’ decays occur at rates which are suppressed by a factor  $\cos^2 \theta_C \approx 0.95$ , while the previously ‘forbidden’ decays are now allowed, but with rates which are suppressed by a factor  $\sin^2 \theta_C \approx 0.05$ .

Historically, the most remarkable thing about these ideas is that they were formulated before the discovery of the charmed quark. In 1971 seven fundamental fermions were known: the four leptons  $\nu_e$ ,  $e^-$ ,  $\nu_\mu$  and  $\mu^-$ , and the three quarks  $u$ ,  $d$  and  $s$ . This led Glashow, Iliopolous and Maiani to propose the existence of a fourth quark  $c$  to complete the lepton–quark symmetry and to solve problems associated with neutral currents that we will discuss in Section 6.7. The existence of the charmed quark was subsequently confirmed in 1974 with the discovery of the first charmonium states (this is why their discovery was so important – see the discussion in Section 5.3) and its measured weak couplings are consistent with the predictions of lepton–quark symmetry and quark mixing.

We now know that there are six leptons

$$\begin{pmatrix} \nu_e \\ e^- \end{pmatrix} \quad \begin{pmatrix} \nu_\mu \\ \mu^- \end{pmatrix} \quad \begin{pmatrix} \nu_\tau \\ \tau^- \end{pmatrix} \quad (6.32)$$

<sup>9</sup>This is yet another example of physical states being mixtures of other states.

and six known quarks

$$\begin{pmatrix} u \\ d \end{pmatrix} \quad \begin{pmatrix} c \\ s \end{pmatrix} \quad \begin{pmatrix} t \\ b \end{pmatrix}. \quad (6.33)$$

When the third generation is taken into account, the mixing scheme becomes more complicated, as we must allow for the possibility of mixing between all three ‘lower’ quarks  $d$ ,  $s$  and  $b$  instead of just the first two and more parameters are involved. In general the mixing can be written in the form

$$\begin{pmatrix} d' \\ s' \\ b' \end{pmatrix} = \begin{pmatrix} V_{ud} & V_{us} & V_{ub} \\ V_{cd} & V_{cs} & V_{cb} \\ V_{td} & V_{ts} & V_{tb} \end{pmatrix} \begin{pmatrix} d \\ s \\ b \end{pmatrix}, \quad (6.34)$$

where  $V_{ij}$  ( $i = u, c, t$ ;  $j = d, s, b$ ) the so-called *CKM matrix*,<sup>10</sup> is unitary to ensure the orthonormality of the new states generated by the transformation. The matrix elements  $V_{ij}$  are all obtainable from various decay processes and values exist for them, although the smaller off-diagonal terms are not very well measured.<sup>11</sup> For the first two generations, the changes introduced by this more complex mixing are very small. However, a new feature that emerges is the possibility of *CP* violation. We shall see in the Section 6.6.1 that *CP* violation does actually occur in the decays of neutral *K*-mesons and neutral *B*-mesons and it is of considerable interest to see if the size of the violation is consistent with the CKM mixing formalism and the standard model.

## 6.5.2 Neutrino scattering

Consider the elastic scattering process  $\nu_e + e^- \rightarrow \nu_e + e^-$  at high energies, proceeding via the exchange of a *W*-meson, i.e. a charged current weak interaction. We know the *W*-meson couples only to left-handed fermions and from the discussion of Section 6.3.1 that neutrinos have negative helicity, i.e. they are polarized along the direction of their motion (which we will take to be the  $z$ -axis). We also know from the work of Section 6.3.2 that in the relativistic limit, the same is true of electrons. We are therefore led to the centre-of-mass spin/momentum configurations before the collision shown in Figure 6.14(a). If the interaction scatters the particles through an angle of  $180^\circ$ , then the centre-of-mass spin/momentum configurations after the collision are those shown in Figure 6.14(b). In

<sup>10</sup>The initials stand for Cabibbo, Kobayashi and Maskawa, the last two of whom extended the original Cabibbo scheme to three generations of quarks.

<sup>11</sup>A review is given Ei04.

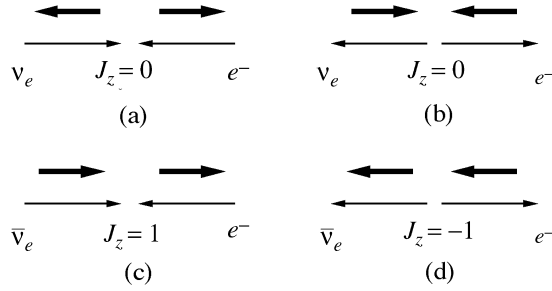


**Figure 6.14** Spin (thick arrows) and momentum (thin arrows) configurations for  $\nu_e e^-$  and  $\bar{\nu}_e e^-$  interactions: (a)  $\nu_e e^-$  before collision; (b)  $\nu_e e^-$  after scattering through  $180^\circ$ ; (c)  $\bar{\nu}_e e^-$  before collision; (d)  $\bar{\nu}_e e^-$  after scattering through  $180^\circ$

both cases the total spin component along the  $z$ -axis is zero. This result is true for all angles and the scattering is isotropic.

From this we can calculate the differential cross-section using the formulae of Chapter 1. We will assume that the squared momentum transfer  $Q^2$  is such that  $Q_{\max}^2 \ll M_W^2 c^2$ , so that the matrix element may be written [cf. Equation (6.1)]

$$f(\nu_e + e^- \rightarrow \nu_e + e^-) = -G_F, \quad (6.35)$$

where  $G_F$  is the Fermi coupling constant of Equation (1.42), i.e.

$$G_F = \frac{4\pi(\hbar c)^3 \alpha_W}{(M_W c^2)^2} \quad (6.36)$$

and  $\alpha_W = g^2/4\pi\hbar c$  is the equivalent of the fine structure constant for charged current weak interactions. Hence, using Equation (1.57) and recalling that the velocities of both the neutrino and electron are equal to  $c$ ,

$$\frac{d\sigma}{d\Omega}(\nu_e e^-) = \frac{1}{4\pi^2} \frac{G_F^2}{(\hbar c)^4} E_{\text{CM}}^2. \quad (6.37)$$

At high energies  $E_{\text{CM}}^2$  is given by

$$E_{\text{CM}}^2 \approx 2m_e c^2 E_\nu, \quad (6.38)$$

where  $E_\nu$  is the energy of the neutrino. So finally the total cross-section is

$$\sigma_{\text{tot}}(\nu_e e^-) = \frac{2m_e c^2 G_F^2}{\pi(\hbar c)^4} E_\nu \quad (6.39)$$

and increases linearly with  $E_\nu$ .<sup>12</sup>

If we apply the same argument to the scattering of antineutrinos, we are led to the configurations shown in Figures 6.14(c) and 6.14(d). The initial state has  $J_z = 1$ , but the final state has  $J_z = -1$ . Thus scattering through  $180^\circ$  is forbidden by angular momentum conservation and the amplitude must contain a factor  $(1 + \cos \theta)$ . This is borne out by a full calculation using the **V-A** formalism which gives, in the same approximation,

$$\frac{d\sigma}{d\Omega}(\bar{\nu}_e e^-) = \frac{1}{16\pi^2} \frac{G_F^2}{(\hbar c)^4} E_{\text{CM}}^2 (1 + \cos \theta)^2. \quad (6.40)$$

Integrating over angles gives

$$\sigma_{\text{tot}}(\bar{\nu}_e e^-) = \frac{1}{3} \sigma_{\text{tot}}(\nu_e e^-). \quad (6.41)$$

Neutrino–electron scattering is not, of course, a very practical reaction to study experimentally, but these ideas may be taken over to deep inelastic neutrino scattering from nucleons, where the latter are assumed to be composed of constituent quarks whose masses may be neglected at high energies. This will enable us to extend the discussion of Section 5.7 for charged leptons. In this case the neutrino is assumed to interact with a single quark within the nucleon (this is again the spectator model) and we must take account of all relevant quarks and antiquarks. In practice we can neglect interactions with  $s$  and  $\bar{s}$  quarks as these will be suppressed by the Cabibbo factor. So, taking into account only the  $u$  and  $d$  quarks and their antiparticles, we can generalize Equations (6.39) and (6.41) to give

$$\sigma_{\text{tot}}(\nu_e N) = \frac{M_N c^2 G_F^2 E_\nu}{\pi (\hbar c)^4} \left( H + \frac{1}{3} \bar{H} \right) \quad (6.42a)$$

and

$$\sigma_{\text{tot}}(\bar{\nu}_e N) = \frac{M_N c^2 G_F^2 E_\nu}{\pi (\hbar c)^4} \left( \frac{1}{3} H + \bar{H} \right), \quad (6.42b)$$

for scattering from an isoscalar nucleus, i.e. one with an equal number of neutrons and protons, where  $M_N$  is the mass of the nucleon. The quantities  $H$  and  $\bar{H}$  are given by

$$H \equiv \int_0^1 x[u(x) + d(x)]dx \quad \text{and} \quad \bar{H} \equiv \int_0^1 x[\bar{u}(x) + \bar{d}(x)]dx, \quad (6.43)$$

<sup>12</sup>This behaviour has arisen because of the approximation Equation (6.35). It cannot of course continue indefinitely. At very high values of  $Q^2$  the full form of the propagator would have to be taken into account and this would introduce an energy dependence in the denominator of Equation (6.39).

where  $u(x)$  etc. are the quark densities defined in Section 5.7 and the integral is over the scaling variable  $x$ .

Setting  $y = \bar{H}/H$ , we have from Equations (6.42)

$$R \equiv \frac{\sigma(\bar{\nu}_e N)}{\sigma(\nu_e N)} = \frac{1 + 3y}{3 + y}. \tag{6.44}$$

Some data for  $R$  are shown in Figure 6.15 from an experiment using muon-neutrinos. These show that  $R$  is approximately constant, as predicted by Equation (6.44), and has a value of about 0.51, which implies  $y \approx 0.2$ , i.e. antiquarks exist in the nucleon at the level of about 20 per cent. Other experiments yield similar results in the range 15–20 per cent.

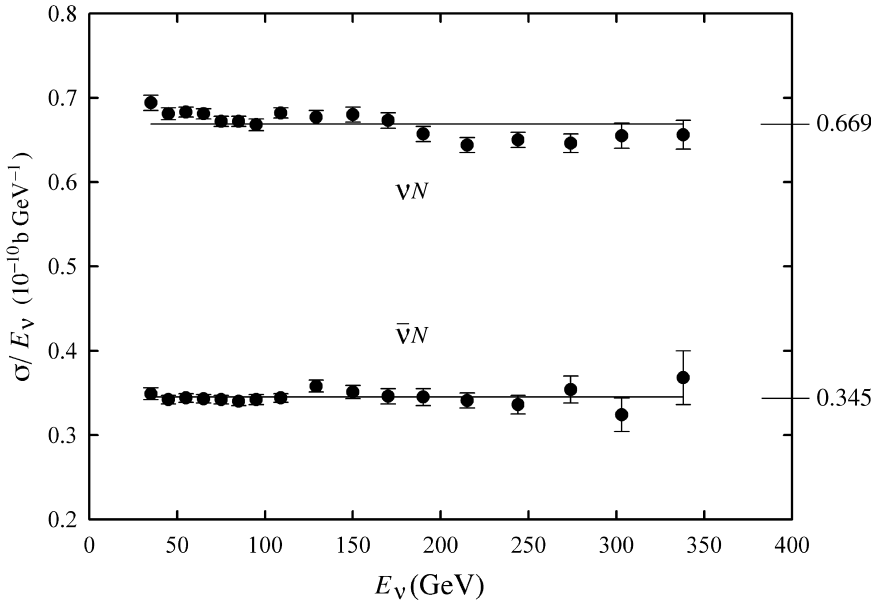


Figure 6.15 Neutrino and antineutrino total cross-sections (data from Se97)

## 6.6 Neutral Meson Decays

Neutral mesons are of particular interest not only because they enable very sensitive tests of  $CP$ -conservation to be made, but also because the application of basic quantum mechanics leads to surprising effects that, for example, allow the symmetry between particles and antiparticles to be tested with extraordinary precision. In both cases the crucial ingredient is the phenomenon of particle mixing that we have met before in connection with the mixing of neutrino flavour

states. Because most work has been done on the neutral kaons, we will mainly discuss this system as an example. The equivalent formalisms for  $B$ - and  $D$ -decays are similar. We start with a discussion of  $CP$  violation.

### 6.6.1 CP violation

We have seen that there are two neutral kaon states

$$K^0(498) = d\bar{s} \quad \text{and} \quad \bar{K}^0(498) = s\bar{d}, \quad (6.45)$$

which have strangeness  $S = +1$  and  $S = -1$  respectively. However, because strangeness is not conserved in weak interactions, these states can be converted into each other by higher-order weak processes like those shown in Figure 6.16.

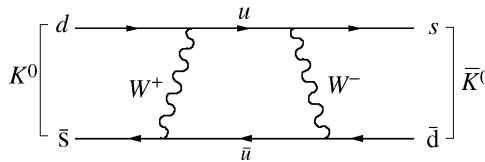


**Figure 6.16** Example of a process that can convert a  $K^0$  state to a  $\bar{K}^0$  state

This is in marked contrast to most other particle–antiparticle systems, for which such transitions are forbidden, because the particle and its antiparticle differ by quantum numbers that are conserved in all known interactions. For example, the  $\pi^+$  and  $\pi^-$  have opposite electric charges, and the neutron and antineutron have opposite baryon numbers. For neutral kaons, however, there is no conserved quantum number to distinguish the  $K^0$  and  $\bar{K}^0$  states when weak interactions are taken into account and the observed physical particles correspond not to the  $K^0$  and  $\bar{K}^0$  states themselves, but to linear combinations of them. Similar mixing can occur between  $B^0 - \bar{B}^0$  and  $D^0 - \bar{D}^0$  states. We have met the idea that observed states can be linear combinations of other states in the CKM mixing scheme for quarks above and earlier when we discussed neutrino oscillations in the absence of lepton number conservation in Chapter 3. In the present case it leads to the phenomena of  $K^0 - \bar{K}^0$  mixing, and *strangeness oscillations*.

We start by assuming that  $CP$ -invariance is exact and that neutral kaons are eigenstates of the combined  $CP$  operator. In this case, using the standard phase convention, we can define

$$C|K^0, \mathbf{p}\rangle = -|\bar{K}^0, \mathbf{p}\rangle, \quad C|\bar{K}^0, \mathbf{p}\rangle = -|K^0, \mathbf{p}\rangle, \quad (6.46)$$

where  $|K^0, \mathbf{p}\rangle$  denotes a  $K^0$  state with momentum  $\mathbf{p}$ , etc.. Since kaons have negative intrinsic parity, we also have for  $\mathbf{p} = \mathbf{0}$

$$P|K^0, \mathbf{0}\rangle = -|K^0, \mathbf{0}\rangle, \quad P|\bar{K}^0, \mathbf{0}\rangle = -|\bar{K}^0, \mathbf{0}\rangle, \quad (6.47)$$

so that

$$CP|K^0, \mathbf{0}\rangle = |\bar{K}^0, \mathbf{0}\rangle, \quad CP|\bar{K}^0, \mathbf{0}\rangle = |K^0, \mathbf{0}\rangle. \quad (6.48)$$

Thus  $CP$  eigenstates  $K_{1,2}^0$  are

$$|K_{1,2}^0, \mathbf{0}\rangle = \frac{1}{\sqrt{2}} \left\{ |K^0, \mathbf{0}\rangle \pm |\bar{K}^0, \mathbf{0}\rangle \right\} \quad (CP = \pm 1). \quad (6.49)$$

If  $CP$  is conserved, then  $K_1^0$  should decay entirely to states with  $CP = 1$  and  $K_2^0$  should decay entirely into states with  $CP = -1$ . We examine the consequences of this for decays leading to pions in the final state.

Consider the state  $\pi^0\pi^0$ . Since the kaon has spin-0, by angular momentum conservation the pion pair must have zero orbital angular momentum in the rest frame of the decaying particle. Its parity is therefore given by [cf. Equation (1.14)]

$$P = P_\pi^2(-1)^L = 1, \quad (6.50)$$

where  $P_\pi = -1$  is the intrinsic parity of the pion. The  $C$ -parity is given by

$$C = (C_{\pi^0})^2 = 1, \quad (6.51)$$

where  $C_{\pi^0} = 1$  is the  $C$ -parity of the neutral pion. Combining these results gives  $CP = 1$ . The same result holds for the  $\pi^+\pi^-$  final state.

The argument for three-pion final states  $\pi^+\pi^-\pi^0$  and  $\pi^0\pi^0\pi^0$  is more complicated, because there are two orbital angular momenta to consider. If we denote by  $\mathbf{L}_{12}$  the orbital angular momentum of one pair (either  $\pi^+\pi^-$  or  $\pi^0\pi^0$ ) in their mutual centre-of-mass frame, and  $\mathbf{L}_3$  is the orbital angular momentum of the third pion about the centre-of-mass of the pair in the overall centre-of-mass frame, then the total orbital angular momentum  $\mathbf{L} \equiv \mathbf{L}_{12} + \mathbf{L}_3 = \mathbf{0}$ , since the decaying particle has spin-0. This can only be satisfied if  $L_{12} = L_3$ . This implies that the parity of the final state is

$$P = P_\pi^3(-1)^{L_{12}}(-1)^{L_3} = -1. \quad (6.52)$$

For the  $\pi^0\pi^0\pi^0$  final state, the  $C$ -parity is

$$C = (C_{\pi^0})^3 = 1 \quad (6.53)$$

and combining these results gives  $CP = -1$  overall. The same result can be shown to hold for the  $\pi^+\pi^-\pi^0$  final state.

The experimental position is that two neutral kaons are observed, called  $K^0$ -short and  $K^0$ -long, denoted  $K_S^0$  and  $K_L^0$ , respectively. They have almost equal masses of about  $499 \text{ MeV}/c^2$ , but very different lifetimes and decay modes. The  $K_S^0$  has a

lifetime of  $0.89 \times 10^{-10}$  s and decays overwhelmingly to two pions; the longer-lived  $K_L^0$  has a lifetime of  $0.52 \times 10^{-7}$  s with a significant branching ratio to three pions, but not to two. In view of the  $CP$  analysis above, this immediately suggests the identification

$$K_S^0 = K_1^0, \quad \text{and} \quad K_L^0 = K_2^0. \quad (6.54)$$

However, in 1964 it was discovered that the  $K_L^0$  also decayed to two pions<sup>13</sup>

$$K_L^0 \rightarrow \pi^+ + \pi^-, \quad (6.55)$$

but with a very small branching ratio of the order of  $10^{-3}$ . This result is clear evidence of  $CP$  violation. This was confirmed in later experiments on the decay  $K^0 \rightarrow \pi^0 \pi^0$ .

Because  $CP$  is not conserved, the physical states  $K_S^0$  and  $K_L^0$  need not correspond to the  $CP$ -eigenstates  $K_1^0$  and  $K_2^0$ , but can contain small components of states with the opposite  $CP$ , i.e. we may write

$$|K_S^0, \mathbf{0}\rangle = \frac{1}{(1 + |\varepsilon|^2)^{1/2}} [ |K_1^0, \mathbf{0}\rangle - \varepsilon |K_2^0, \mathbf{0}\rangle ] \quad (6.56a)$$

and

$$|K_L^0, \mathbf{0}\rangle = \frac{1}{(1 + |\varepsilon|^2)^{1/2}} [ \varepsilon |K_1^0, \mathbf{0}\rangle + |K_2^0, \mathbf{0}\rangle ], \quad (6.56b)$$

where  $\varepsilon$  is a small complex parameter. (The factor in front of the brackets is to normalize the states.) The  $CP$ -violating decays can then occur in two different ways: either (a) the  $CP$ -forbidden  $K_1^0$  component in the  $K_L^0$  decays via a  $CP$ -allowed process, giving a contribution proportional to the probability  $|\varepsilon|^2 [1 + |\varepsilon|^2]^{-1} \approx |\varepsilon|^2$  of finding a  $K_1^0$  component in the  $K_L^0$ ; or (b) the  $CP$ -allowed  $K_2^0$  component in the  $K_L^0$  decays via a  $CP$ -violating reaction. A detailed analysis of the data for the  $\pi\pi$  decay modes<sup>14</sup> shows that it is the former mechanism that dominates, with  $|\varepsilon| \approx 2.2 \times 10^{-3}$ .

This is confirmed in the semileptonic decays

$$K^0 \rightarrow \pi^- + e^+ + \nu_e \quad (6.57a)$$

<sup>13</sup>The experiment was led by James Cronin and Val Fitch. They received the 1980 Nobel Prize in Physics for their discovery.

<sup>14</sup>See, for example, Ei04.

and

$$\bar{K}^0 \rightarrow \pi^+ + e^- + \bar{\nu}_e. \tag{6.57b}$$

For example, if we start with a beam of  $K^0$  particles, with initially equal amounts of  $K_S^0$  and  $K_L^0$ , then after a time that is large compared with the  $K_S^0$  lifetime, the  $K_S^0$  component will have decayed leaving just the  $K_L^0$  component, which itself will be an equal admixture of  $K^0$  and  $\bar{K}^0$  components. We would therefore expect to observe identical numbers of electrons ( $N^-$ ) and positrons ( $N^+$ ) from the decays of Equations (6.57). However, if  $K_L^0$  is not an eigenstate of  $CP$ , then there will be an asymmetry in these numbers, which will depend on the relative strengths of the  $K^0$  and  $\bar{K}^0$  components in  $K_L^0$ . The asymmetry is given by  $2\text{Re}\varepsilon$ , where  $\varepsilon$  is the  $CP$ -violating parameter defined in Equation (6.56).

Figure 6.17 shows data on the asymmetry  $(N^+ - N^-)/(N^+ + N^-)$  as a function of proper time. After the initial oscillations there is seen to be an asymmetry whose value is  $2\text{Re}\varepsilon \approx 3.3 \times 10^{-3}$ , which is consistent with the value of  $\varepsilon$  obtained from the  $\pi\pi$  modes. Thus  $CP$ -violation in  $K$ -decay occurs mainly, though not entirely, by the mixing of the  $CP$ -eigenstates in the physical states rather than by direct  $CP$ -violating decays, both of which are allowed in the CKM mixing scheme.

What do these results mean for the CKM mixing scheme? The CKM matrix is a  $3 \times 3$  matrix and in general contains nine complex elements. However, the unitary nature of the matrix implies that there are relations between the elements, such as

$$V_{ud}V_{ub}^* + V_{cd}V_{cb}^* + V_{td}V_{tb}^* = 0. \tag{6.58}$$

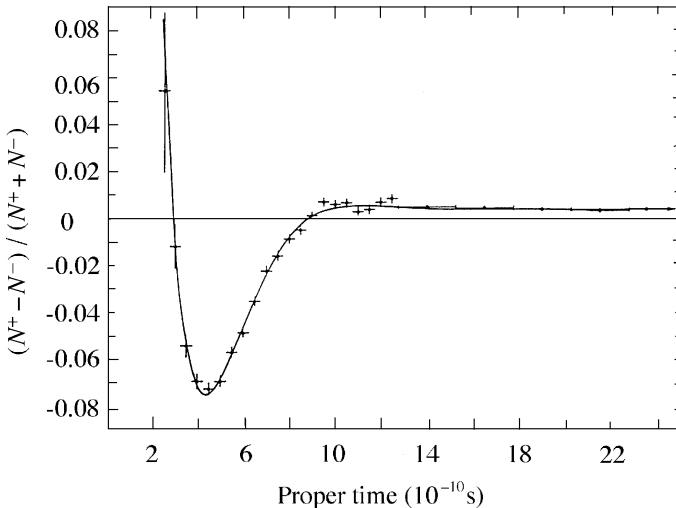


**Figure 6.17** The charge asymmetry observed for  $K^0 \rightarrow \pi^- e^+ \nu_e$  and  $\bar{K}^0 \rightarrow \pi^+ e^- \bar{\nu}_e$  as a function of proper time, for a beam that is initially predominantly  $K^0$  (adapted from Gj74, copyright Elsevier, with permission)

Using these and exploiting the freedom to define the phases of the basic quark states, the matrix may be parameterized by just four quantities. A number of different parameterizations are used, but an approximate form that is commonly used to discuss  $CP$  violation is

$$V = \begin{pmatrix} 1 - \frac{1}{2}\lambda^2 & \lambda & A\lambda^3(\rho - i\eta) \\ -\lambda & 1 - \frac{1}{2}\lambda^2 & A\lambda^2 \\ A\lambda^3(1 - \rho - i\eta) & -A\lambda^2 & 1 \end{pmatrix} + O(\lambda^4), \quad (6.59)$$

with parameters  $A$ ,  $\lambda$ ,  $\rho$  and  $\eta$ . The quantity  $\lambda = |V_{us}| \approx 0.22$  plays the role of an expansion parameter in this approximation and a non-zero value of  $\eta$  would be indicative of  $CP$  violation.

The parameter  $\varepsilon$  in Equations (6.56) is just one  $CP$ -violating parameter that may be measured in various  $K$ -decay modes. We will not pursue this further, but note that by combining the values of the parameters with information on other elements of the CKM matrix, a value of the  $CP$ -violating parameter  $\eta$  may be deduced and used to predict the size of  $CP$ -violating effects in other decays. There are very few other places where such mixing effects can occur, but in principle they should be possible in the  $D^0\bar{D}^0$  and  $B^0\bar{B}^0$  systems, which are analogues of the  $K$ -mesons, but with a strange quark replaced by a charmed and bottom quark, respectively. Mixing in the  $B^0\bar{B}^0$  states due to  $B^0\bar{B}^0$  oscillations has in fact been observed and also very recently direct  $CP$  violation. The latter was established by comparing the decay  $B^0 \rightarrow K^+\pi^-$  with the decay  $\bar{B}^0 \rightarrow K^-\pi^+$ . Moreover, the size of the effect is much stronger than in neutral kaon decays and this is in agreement with the predictions of the CKM mixing scheme.

There is still much to be done in studying  $CP$  violation. For example, the cleanest measurement of the  $CP$ -violating parameter would be from the decays  $B^0/\bar{B}^0 \rightarrow (J/\psi)K_S^0$ , where  $J/\psi$  is the  $^3S_1$  ground state of charmonium, but the present limits on these decays are orders of magnitude from those required to test the predictions. On the theoretical side, although the CKM mixing model accounts for all  $CP$ -violating data to date, it fails by several orders of magnitude to account for the observed matter–antimatter asymmetry observed in the universe (which will be discussed in Chapter 9) and so there is probably a  $CP$ -violating mechanism beyond the standard model awaiting to be discovered.

## 6.6.2 Flavour oscillations

One interesting consequence of flavour mixing for the  $K^0 - \bar{K}^0$  system is the phenomenon of *strangeness oscillation*, which occurs whenever a neutral kaon is produced in a strong interaction process. For example, the neutral kaon produced in the strong interaction

$$\begin{aligned} \pi^- + p &\rightarrow K^0 + \Lambda^0 \\ S &= 0 \quad 0 \quad 1 \quad -1 \end{aligned} \quad (6.60)$$

must necessarily be a  $K^0$  state with  $S = 1$ , in order to conserve strangeness. However, if the produced particle is allowed to travel through free space and its strangeness is measured, one finds that it no longer has a definite strangeness  $S = 1$ , but has components with both  $S = 1$  and  $S = -1$  whose intensities oscillate with time. These are called strangeness oscillations. The phenomenon is very similar mathematically to that describing the flavour oscillations of neutrinos we met in Chapter 3 and enables the mass difference between  $K_S^0$  and  $K_L^0$  particles to be measured with extraordinary precision, as we will now show.

In what follows, we shall measure time in the rest frame of the produced particle, and define  $t = 0$  as the moment when it is produced. If we ignore the very small  $CP$  violations, the initial state produced in the  $\pi^- p$  reaction above is

$$|K^0, \mathbf{p}\rangle = \frac{1}{\sqrt{2}} \{ |K_S^0, \mathbf{p}\rangle + |K_L^0, \mathbf{p}\rangle \}. \quad (6.61)$$

At later times, however, this will become

$$\frac{1}{\sqrt{2}} \{ a_S(t) |K_S^0, \mathbf{p}\rangle + a_L(t) |K_L^0, \mathbf{p}\rangle \}, \quad (6.62)$$

where

$$a_\alpha(t) = e^{-im_\alpha t} e^{-\Gamma_\alpha t/2} \quad (\alpha = S, L) \quad (6.63)$$

and  $m_\alpha$  and  $\Gamma_\alpha$  are the mass and decay rate of the particle concerned. Here the first exponential factor is the usual oscillating time factor  $e^{-iEt}$  associated with any quantum mechanical stationary state, evaluated in the rest frame of the particle. The second exponential factor reflects the fact that the particles decay, and it ensures that the probability

$$\left| \frac{1}{\sqrt{2}} a_\alpha(t) \right|^2 = \frac{1}{2} e^{-\Gamma_\alpha t} \quad (\alpha = S, L) \quad (6.64)$$

of finding a  $K_S^0$  or  $K_L^0$  decreases exponentially with a mean lifetime  $\tau_\alpha = \Gamma_\alpha^{-1}$  ( $\alpha = S, L$ ). Because  $\tau_S \ll \tau_L$ , for times  $t$  such that  $\tau_S \ll t \lesssim \tau_L$  only the  $K_L^0$  component survives, implying equal intensities for the  $K^0$  and  $\bar{K}^0$  components. Here we are interested in the intensities of the  $K^0$  and  $\bar{K}^0$  components at shorter times, and to deduce these we rewrite the expression

$$\frac{1}{\sqrt{2}} \{ a_S(t) |K_S^0, \mathbf{p}\rangle + a_L(t) |K_L^0, \mathbf{p}\rangle \} \quad (6.65)$$

in the form

$$\{ A_0(t) |K^0, \mathbf{p}\rangle + \bar{A}_0(t) |\bar{K}^0, \mathbf{p}\rangle \}, \quad (6.66)$$

where

$$A_0(t) = \frac{1}{2}[a_S(t) + a_L(t)] \quad \text{and} \quad \bar{A}_0(t) = \frac{1}{2}[a_S(t) - a_L(t)]. \quad (6.67)$$

The intensities of the two components are then given by

$$I(K^0) \equiv |A_0(t)|^2 = \frac{1}{4} \left[ e^{-\Gamma_S t} + e^{-\Gamma_L t} + 2e^{-(\Gamma_S + \Gamma_L)t/2} \cos(\Delta m t) \right] \quad (6.68a)$$

and

$$I(\bar{K}^0) \equiv |\bar{A}_0(t)|^2 = \frac{1}{4} \left[ e^{-\Gamma_S t} + e^{-\Gamma_L t} - 2e^{-(\Gamma_S + \Gamma_L)t/2} \cos(\Delta m t) \right] \quad (6.68b)$$

where  $\Delta m \equiv |m_S - m_L|$  and we have used Equation (6.63) explicitly to evaluate the amplitudes.

The variation of the  $\bar{K}^0$  intensity  $I(\bar{K}^0)$  with time can be determined experimentally by measuring the rate of production of *hyperons* (baryons with non-zero strangeness) in strangeness-conserving strong interactions such as



as a function of the distance from the  $K^0$  source. The data are then fitted by Equations (6.68) with  $\Delta m$  as a free parameter and the predictions are in good agreement with the experiments for a mass difference

$$\Delta m = (3.522 \pm 0.016) \times 10^{-12} \text{ MeV}/c^2. \quad (6.70)$$

The states  $K_S^0$  and  $K_L^0$  are not antiparticles but the  $K^0$  and  $\bar{K}^0$  are, of course, and the mass difference  $\Delta m$  can be shown to arise solely from the possibility of transitions  $K \leftrightarrow \bar{K}^0$ , whose magnitude can be calculated from diagrams like that shown in Figure 6.16. We shall not discuss this further, but merely note that the resulting agreement between the predicted and measured values confirms the equality  $m_{K^0} = m_{\bar{K}^0}$  to better than one part in  $10^{17}$ . (This should be compared with the next most precisely tested particle–antiparticle mass relation  $m_{e^+} = m_{e^-}$  which only verified to within an experimental error of the order of one part in  $10^7$ .) This equality is a prediction of the so-called *CPT theorem*, which states that under very general conditions any relativistic quantum theory will be invariant under the combined operations of  $C$ ,  $P$  and  $T$ .

## 6.7 Neutral Currents and the Unified Theory

Neutral current reactions are those that involve the emission, absorption or exchange of  $Z^0$  bosons. The unified electroweak theory predicted the existence

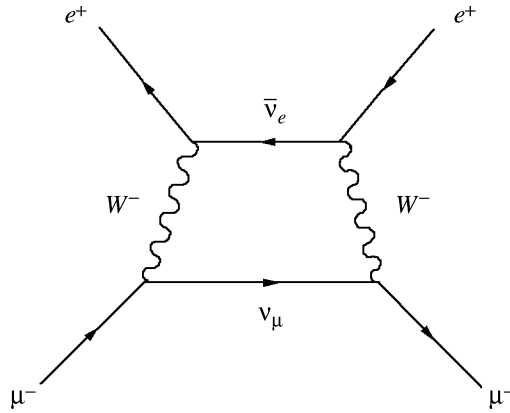


**Figure 6.18** Higher order contribution to the reaction  $e^+\mu^- \rightarrow e^+\mu^-$  from the exchange of two  $W$ -bosons

of such reactions before their discovery in 1973. This theory<sup>15</sup> was proposed mainly in order to solve problems associated with Feynman diagrams in which more than one  $W$  boson was exchanged, like that shown in Figure 6.18, which contributes to the reaction  $e^+\mu^- \rightarrow e^+\mu^-$ .

Such contributions are expected to be small because they are higher order in the weak interaction and this appears to be confirmed by experimental data, which are in good agreement with theoretical predictions that neglect them entirely. (For example, in the experimentally accessible reaction  $e^+ + e^- \rightarrow \mu^+ + \mu^-$ .) However, when these higher-order contributions are explicitly calculated, they are found to be proportional to divergent integrals, i.e. they are infinite. In the unified theory, this problem is solved when diagrams involving the exchange of  $Z^0$  bosons and photons are taken into account. These also give infinite contributions, but when all the diagrams of a given order are added together the divergences cancel (!), giving a well-defined and finite contribution overall.<sup>16</sup> This cancellation is not accidental, but is a consequence of a fundamental symmetry relating the weak and electromagnetic interactions. Here we will simply comment on some phenomenological consequences of the theory.

<sup>15</sup>The formulation of the theory is in terms of four massless vector bosons arranged as multiplets of ‘weak isospin’ and ‘weak hypercharge’. Specifically, three states are a weak isospin triplet and the fourth is a weak isospin singlet. The fact that they all have zero masses ensures that gauge invariance is satisfied. These fields then interact with additional scalar fields associated with new postulated particles called Higgs bosons, which we have mentioned elsewhere. This process, known as ‘spontaneous symmetry breaking’ generates the observed masses of the  $W$ ,  $Z$  and  $\gamma$  bosons, while still preserving gauge invariance. (For further details see, for example, Section 8.4 of Pe00.) The originators of this theory, Sheldon Glasow, Abdus Salam and Steven Weinberg, shared the 1979 Nobel Prize in Physics for their contributions to formulating the electroweak theory and the prediction of weak neutral currents.

<sup>16</sup>The first people to demonstrate that this occurred were Gerardus ‘t Hooft and Martinus Veltman. They shared the 1999 Nobel Prize in Physics for this discovery.

The first is that to ensure the cancellation, the theory requires a relation between the weak and electromagnetic couplings, called the *unification condition*. This is

$$\frac{e}{2\sqrt{2}\varepsilon_0^{1/2}} = g_w \sin \theta_W = g_z \cos \theta_W, \quad (6.71)$$

where the *weak mixing angle*  $\theta_W$  (also called the *Weinberg angle* after one of the authors of the theory) is given by

$$\cos \theta_W \equiv M_W/M_Z \quad (0 < \theta < \pi/2) \quad (6.72)$$

and  $g_z$  is a coupling constant which characterizes the strength of the neutral current vertices. The unification condition relates the strengths of the various interactions to the  $W$  and  $Z$  masses, and historically was used to predict the latter from the former before the  $W^\pm$  and  $Z^0$  bosons were discovered.

Secondly, just as all the charged current interactions of leptons can be understood in terms of the basic  $W^\pm$ -lepton vertices, in the same way all known neutral current interactions can be accounted for in terms of basic  $Z^0$ -lepton vertices shown in Figures 6.19(a) and 6.19(b). The corresponding quark vertices can be obtained from the lepton vertices by using lepton-quark symmetry and quark mixing, in the same way that  $W^\pm$ -quark vertices are obtained from the  $W^\pm$ -lepton vertices. Thus, making the replacements

$$\nu_e \rightarrow u, \quad \nu_\mu \rightarrow c, \quad e^- \rightarrow d', \quad \mu^- \rightarrow s' \quad (6.73)$$

in the lepton vertices

$$\nu_e \nu_e Z^0, \quad \nu_\mu \nu_\mu Z^0, \quad e^- e^- Z^0, \quad \mu^- \mu^- Z^0, \quad (6.74)$$

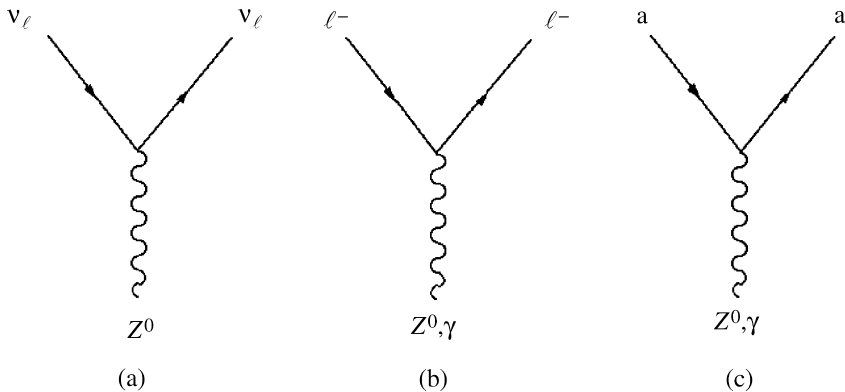


**Figure 6.19**  $Z^0$  and  $\gamma$  couplings to leptons and quarks in the unified electroweak theory, where  $\ell = e, \mu$  and  $\tau$  and  $a$  denotes a quark

leads to the quark vertices

$$uuZ^0, \quad ccZ^0, \quad d'd'Z^0, \quad s's'Z^0. \quad (6.75)$$

Finally, we interpret the latter two of these using Equations (6.30). Thus, for example,

$$\begin{aligned} d'd'Z^0 &= (d \cos \theta_C + s \sin \theta_C) (d \cos \theta_C + s \sin \theta_C) Z^0 \\ &= ddZ^0 \cos^2 \theta_C + ssZ^0 \sin^2 \theta_C + (dsZ^0 + sdZ^0) \sin \theta_C \cos \theta_C \end{aligned} \quad (6.76)$$

When all the terms in Expression (6.75) are evaluated, ones obtains a set of vertices equivalent to

$$uuZ^0, \quad ccZ^0, \quad ddZ^0, \quad ssZ^0, \quad (6.77)$$

which are shown in Figure 6.19(c).

One important difference from charged current reactions that follows from Figure 6.19 is that neutral current interactions *conserve* individual quark numbers. Thus, for example, strangeness-changing weak neutral current reactions are forbidden. An example is the decay  $K^0 \rightarrow \mu^+ \mu^-$  and indeed this is not seen experimentally, although nothing else forbids it.

It follows from the above that in any process in which a photon is exchanged, a  $Z^0$  boson can be exchanged as well. At energies that are small compared with the  $Z^0$  mass, the  $Z^0$ -exchange contributions can be neglected compared to the corresponding photon exchange contributions, and these reactions can be regarded as purely electromagnetic to a high degree of accuracy. However, at very high energy and momentum transfers,  $Z^0$ -exchange contributions become comparable with those of photon exchange and we are therefore dealing with genuinely electroweak processes which involve both weak and electromagnetic interactions to a comparable degree.

These points are clearly illustrated by the cross-section for the muon pair production reaction  $e^+ + e^- \rightarrow \mu^+ + \mu^-$ . If we assume that the energy is large enough for the lepton masses to be neglected, then the centre-of-mass energy  $E$  is the only quantity in the system that has dimensions. Because a cross-section has the dimensions of area, on dimensional grounds the electromagnetic cross-section for one-photon exchange is of the form  $\sigma_\gamma \approx \alpha^2 (\hbar c)^2 / E^2$ . For  $Z^0$ -exchange with  $E \ll M_Z c^2$ , a similar argument gives for the weak interaction cross-section  $\sigma_Z \approx \alpha_Z^2 E^2 (\hbar c)^2 / (M_Z c^2)^4$ . (The factor in the denominator comes from the propagator of the  $Z^0$ -boson.) Thus the one-photon exchange diagram dominates at low energies, and the cross-section falls as  $E^{-2}$ . This is in agreement with the observed behaviour shown in Figure 6.20 and justifies our neglect of the  $Z^0$ -exchange contribution at low energies. However, the relative importance of the  $Z^0$ -exchange contribution increases rapidly with energy and at beam energies of about 35 GeV it

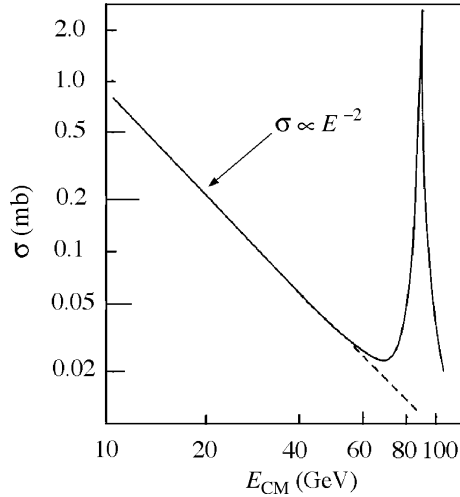


**Figure 6.20** Total cross-section for the reaction  $e^+e^- \rightarrow \mu^+\mu^-$

begins to make a significant contribution to the total cross-section. At still higher energies, the cross-section is dominated by a very large peak at an energy corresponding to the  $Z^0$  mass, as illustrated in Figure 6.20. At this energy the low-energy approximation is irrelevant and Figure 6.20 corresponds to the formation of physical  $Z^0$  bosons in the process  $e^+ + e^- \rightarrow Z^0$  followed by the subsequent decay  $Z^0 \rightarrow \mu^+ + \mu^-$  to give the final-state muons. Finally, beyond the peak we once again regain the electroweak regime where both contributions are comparable.

If the exchange of a  $Z^0$  boson always accompanies the exchange of a photon, then there will also in principle be parity-violating effects in reactions that at first sight we would expect to be purely electromagnetic. Their observation would be further unambiguous evidence for electroweak unification. This was first tested in 1978 by scattering polarized electrons from a deuterium target and measuring the parity-violating asymmetry

$$A_{\text{PV}} \equiv \frac{\sigma_{\text{R}} - \sigma_{\text{L}}}{\sigma_{\text{R}} + \sigma_{\text{L}}}, \quad (6.78)$$

where  $\sigma_{\text{R}}(\sigma_{\text{L}})$  is the cross-section for incident right (left)-handed electrons. To produce polarized electrons is a complicated multistage process that starts with linearly polarized photons from a laser source that are then converted to states with circular polarization. Finally these are used to pump a GaAs crystal (photocathode) to produce the require electrons. Polarizations of about 80 per cent are obtained by this means. The asymmetry is very small and in this experiment  $A_{\text{PV}}$  is predicted to be only a few parts per million. Nevertheless, a non-zero value was definitely established. Moreover,  $A_{\text{PV}}$  was also measured as a function of the fractional energy loss of the initial electron. This is a function of the weak mixing angle and a

value was found in agreement with other determinations, e.g. from deep inelastic neutrino scattering. A later experiment confirmed the effect in polarized electron–proton scattering.

A very recent experiment (2004) has measured  $A_{PV}$  for  $e^-e^-$  scattering. This was done using electrons of about 50 GeV primary energy from the SLAC linear accelerator in Stanford, USA, and scattering them from a liquid hydrogen target. The experiment was able to distinguish final-state electrons scattered from the atomic electrons from those scattered from protons. Taking account of all sources of error, the measured value was  $A_{PV} = (-175 \pm 40) \times 10^{-9}$  (note the exponent – parts per billion) and the experiment also yielded a value of  $\sin^2 \theta_W$  consistent with other determinations. These remarkable experiments provide unambiguous evidence for parity violation in ‘electromagnetic’ processes at the level predicted by theory and hence for the electroweak unification as specified in the standard model.<sup>17</sup>

It should also in principle be possible to detect parity violating effects in atomic physics, where the electromagnetic interactions of the electrons dominate. For example, measurements have been made of the slight change in the polarization angle of light passing through a vapour of metallic atoms. In this case the rotation angle is extremely small ( $\sim 10^{-7}$  rad), but very sensitive experiments can measure the effect to an accuracy of  $\sim 1$  per cent. However, to predict the size of the effects requires a detailed knowledge of the atomic theory of the atom and in all cases to date the uncertainties on the predictions are such that a null effect cannot be ruled out. Thus at present, atomic physics does not compete with particle physics experiments in detecting parity-violating effects and measuring  $\sin^2 \theta_W$ , although this could change in the future.

## Problems

- 6.1** Define charged and neutral current reactions in weak interactions and give an example of each in symbol form. How do they differ in respect of conservation of the strangeness quantum number? Why does observation of the process  $\bar{\nu}_\mu + e^- \rightarrow \bar{\nu}_\mu + e^-$  constitute unambiguous evidence for weak neutral currents, whereas the observation of  $\bar{\nu}_e + e^- \rightarrow \bar{\nu}_e + e^-$  does not?
- 6.2** The reaction  $e^+e^- \rightarrow \mu^+\mu^-$  is studied using colliding beams each of energy 7 GeV and at these energies the reaction is predominantly electromagnetic. Draw its lowest order Feynman diagram. The differential cross-section is given by

$$\left(\frac{d\sigma}{d\Omega}\right) = \frac{\alpha^2 \hbar^2 c^2}{4E_{CM}^2} (1 + \cos^2 \theta),$$

<sup>17</sup>Incidentally, all these experiments are of the fixed-target type, showing that this type of experiment still has a lot to offer.

where  $E_{\text{CM}}$  is the total centre-of-mass energy and  $\theta$  is the scattering angle with respect to the beam direction. Calculate the total cross-section in nanobarns at this energy.

The weak interaction also contributes to this process. Draw the corresponding lowest-order Feynman diagram. The weak interaction adds an *additional* term to the differential cross-section of the form

$$\left(\frac{d\sigma}{d\Omega}\right) = \frac{\alpha^2 \hbar^2 c^2}{4E_{\text{CM}}^2} C_{\text{wk}} \cos \theta.$$

The constant  $C_{\text{wk}}$  may be determined experimentally by measuring the ‘forward-backward’ asymmetry, defined by

$$A_{\text{FB}} = \frac{\sigma_{\text{F}} - \sigma_{\text{B}}}{\sigma_{\text{F}} + \sigma_{\text{B}}},$$

where  $\sigma_{\text{F}}(\sigma_{\text{B}})$  is the total cross-section for scattering in the forward (backward) hemisphere, i.e.  $0 \leq \cos \theta \leq 1$  ( $-1 \leq \cos \theta \leq 0$ ). Derive a relation between  $C_{\text{wk}}$  and  $A_{\text{FB}}$ .

- 6.3** Draw a Feynman diagram at the quark level for the decay  $\Lambda \rightarrow p + \pi^-$ . If nature were to double the weak coupling constant and decrease the mass of the  $W$  boson by a factor of four, what would be the effect on the decay rate  $\Gamma(\Lambda \rightarrow p + \pi^-)$ ?
- 6.4** Neglecting the electron mass, the energy spectrum for the electrons emitted in muon decay is given by

$$\frac{d\omega}{dE_e} = \frac{2G_{\text{F}}^2(m_{\mu}c^2)^2 E_e^2}{(2\pi)^3(\hbar c)^6} \left(1 - \frac{4E_e}{3m_{\mu}c^2}\right).$$

What is the most probable energy for the electron? Draw a diagram showing the orientation of the momenta of the three outgoing particles and their helicities for the case when  $E_e \approx m_{\mu}c^2/2$ . Show also the helicity of the muon. Integrate the energy spectrum to obtain an expression for the total decay width of the muon. Hence calculate the muon lifetime in seconds ( $G_{\text{F}}/(\hbar c)^3 = 1.166 \times 10^{-5} \text{ GeV}^{-2}$ ).

- 6.5** Use lepton universality and lepton-quark symmetry to estimate the branching ratios for (a) the decays  $b \rightarrow c + e^- + \bar{\nu}_e$  (where the  $b$  and  $c$  quarks are bound in hadrons) and (b)  $\tau^- \rightarrow e^- + \bar{\nu}_e + \nu_{\tau}$ . Ignore final states that are Cabibbo-suppressed relative to the lepton modes.
- 6.6** The couplings of the  $Z^0$  to right-handed (R) and left-handed (L) fermions are given by

$$g_{\text{R}}(f) = -q_f \sin^2 \theta_{\text{W}}, \quad g_{\text{L}}(f) = \pm 1/2 - q_f \sin^2 \theta_{\text{W}},$$

where  $q_f$  is the electric charge of the fermion  $f$  in units of  $e$  and  $\theta_{\text{W}}$  is the weak mixing angle. The positive sign in  $g_{\text{L}}$  is used for neutrinos and the  $q = u, c, t$

quarks; the negative sign is used for charged leptons and the  $q = d, s, b$  quarks. If the partial width for  $Z^0 \rightarrow f\bar{f}$  is given by

$$\Gamma_f = \frac{G_F M_Z^3 c^6}{3\pi\sqrt{2}(\hbar c)^3} [g_R^2(f) + g_L^2(f)],$$

calculate the partial widths to neutrinos  $\Gamma_\nu$  and to  $q\bar{q}$  pairs  $\Gamma_q$  and explain the relation of  $\Gamma_q$  to the partial width to hadrons  $\Gamma_{\text{hadron}}$ .

The widths to hadrons and to charged leptons are measured to be  $\Gamma_{\text{had}} = (1738 \pm 12)$  MeV and  $\Gamma_{\text{lep}} = (250 \pm 2)$  MeV, and the total width to all final states is measured to be  $\Gamma_{\text{tot}} = (2490 \pm 7)$  MeV. Use these experimental results and your calculated value for the decay width to neutrinos to show that there are only three generations of neutrinos with masses  $M_\nu < M_Z/2$ .

- 6.7** Explain, with the aid of Feynman diagrams, why the decay  $D^0 \rightarrow K^- + \pi^+$  can occur as a charged-current weak interaction at lowest order, but the decay  $D^+ \rightarrow K^0 + \pi^+$  cannot.
- 6.8** Why is the decay rate of the charged pion much smaller than that of the neutral pion? Draw Feynman diagrams to illustrate your answer.
- 6.9** Draw the lowest-order Feynman diagrams for the decays  $\pi^- \rightarrow \mu^- + \bar{\nu}$  and  $K^- \rightarrow \mu^- + \bar{\nu}_\mu$ . Use lepton–quark symmetry and the Cabibbo hypothesis with the Cabibbo angle  $\theta_C = 12^\circ$  to estimate the ratio

$$R \equiv \frac{\text{Rate}(K^- \rightarrow \mu^- + \bar{\nu}_\mu)}{\text{Rate}(\pi^- \rightarrow \mu^- + \bar{\nu}_\mu)},$$

ignoring all kinematic and spin effects. Comment on your result.

- 6.10** Estimate the ratio of decay rates

$$R \equiv \frac{\Gamma(\Sigma^- \rightarrow n + e^- + \bar{\nu}_e)}{\Gamma(\Sigma^- \rightarrow \Lambda + e^- + \bar{\nu}_e)}$$

and explain why the decay  $\Gamma(\Sigma^+ \rightarrow n + e^+ + \nu_e)$  has never been seen.

- 6.11** One way of looking for the Higgs boson  $H$  is in the reaction  $e^+e^- \rightarrow Z^0H$ . If this reaction is studied at a centre-of-mass energy of 500 GeV in a collider operating for  $10^7$  s per year and the cross-section at this energy is 60 fb, what instantaneous luminosity (in units of  $\text{cm}^{-2}\text{s}^{-1}$ ) would be needed to collect 2000 events in one year if the detection efficiency is 10 per cent. For a Higgs boson with mass  $M_H < 120$  GeV, the branching ratio for  $H \rightarrow b\bar{b}$  is predicted to be 85 per cent. Why will looking for  $b$  quarks help distinguish  $e^+e^- \rightarrow Z^0H$  from the background reaction  $e^+e^- \rightarrow Z^0Z^0$ ?
- 6.12** Hadronic strangeness-changing weak decays approximately obey the so-called ‘ $\Delta I = \frac{1}{2}$  rule’, i.e. the total isospin changes by  $\frac{1}{2}$  in the decay. By assuming a

fictitious strangeness zero  $I = \frac{1}{2}$  particle  $S^0$  in the initial state, find the prediction of this rule for the ratio

$$R \equiv \frac{\Gamma(\Xi^- \rightarrow \Lambda + \pi^-)}{\Gamma(\Xi^0 \rightarrow \Lambda + \pi^0)}.$$

Assume that the state  $|\Xi^0, S^0\rangle$  is an equal mixture of states with  $I = 0$  and  $I = 1$ .

- 6.13** The charged-current differential cross-sections for  $\nu$  and  $\bar{\nu}$  scattering from a spin- $\frac{1}{2}$  target are given by generalizations of Equations (6.37) and (6.40) and may be written

$$\frac{d\sigma^{\text{CC}}(\nu)}{dy} = \frac{1}{\pi} \frac{G^2 H s}{(\hbar c)^4}, \quad \frac{d\sigma^{\text{CC}}(\bar{\nu})}{dy} = \frac{d\sigma^{\text{CC}}(\nu)}{dy} (1-y)^2,$$

where  $s = E_{\text{CM}}^2$ ,  $y = \frac{1}{2}(1 - \cos\theta)$  and  $H$  is the integral of the quark density for the target (cf. Equation (6.43)). The corresponding cross-sections for neutral current scattering are

$$\begin{aligned} \frac{d\sigma^{\text{NC}}(\nu)}{dy} &= \frac{d\sigma^{\text{CC}}(\nu)}{dy} [g_L^2 + g_R^2(1-y)^2], \\ \frac{d\sigma^{\text{NC}}(\bar{\nu})}{dy} &= \frac{d\sigma^{\text{CC}}(\nu)}{dy} [g_L^2(1-y)^2 + g_R^2], \end{aligned}$$

where the right- and left-hand couplings to  $u$  and  $d$  quarks are given by

$$\begin{aligned} g_L(u) &= \frac{1}{2} - \frac{2}{3} \sin^2 \theta_W, & g_R(u) &= -\frac{2}{3} \sin^2 \theta_W, \\ g_L(d) &= -\frac{1}{2} + \frac{1}{3} \sin^2 \theta_W, & g_R(d) &= \frac{1}{3} \sin^2 \theta_W. \end{aligned}$$

Derive expressions for the ratios  $\sigma^{\text{NC}}(\nu)/\sigma^{\text{CC}}(\nu)$  and  $\sigma^{\text{NC}}(\bar{\nu})/\sigma^{\text{CC}}(\bar{\nu})$  in the case of an isoscalar target consisting of valence  $u$  and  $d$  quarks only.